

## Design and analysis of drive module for small-diameter pipeline inspection robot

Heng Cheng <sup>1</sup>, Donglin Tang <sup>1,\*</sup>, Caiying Zhang <sup>2</sup>, Zhang Long <sup>1</sup>

<sup>1</sup> School of Mechanical and Electrical Engineering, Southwest Petroleum University, Chengdu 610500, China;

<sup>2</sup> CNPC National Engineering Research Center for Oil and Gas Drilling Equipment, Chengdu 610000, China;

\* Donglin Tang

### Abstract

Aiming at the detection requirement of DN100 pipeline in oil and gas gathering and transportation station, a small-diameter pipeline robot is designed to study its pipeline trafficability in elbow and vertical pipes. Firstly, according to the characteristics of the pipeline system, combined with worm gear and spring mechanism, the drive module with variable diameter ability is designed. Secondly, the kinematic model of the robot was established, and the geometric constraint analysis and motion analysis were carried out. Then, the robot drive module is analyzed through 3D modeling and simulation software. Finally, a robot pipeline test platform is built for experimental verification. The results show that the robot can walk normally in the vertical pipe, and can pass through the 90° pipe with a curvature radius of 1.5 times the pipe diameter.

### Keywords

Pipeline robot, dynamics simulation, prototype experiment.

### 1. Introduction

In the pipeline system of oil and gas gathering and transmission stations, the transported medium is mostly acidic gas or liquid, which will cause corrosion and other damage to the inner wall of the pipeline. If pipes leak, it will cause a great loss to the economy and endanger personal safety, so it is necessary to conduct defect inspections regularly to ensure the safe transportation of the pipeline. As the pipeline is installed at a high place and the pipe diameter space is small, it is very difficult to manually inspect the internal defects or damage to the pipeline. Therefore, the design of a small diameter pipeline inspection robot instead of a manual, can ensure personal safety, but also ensure the efficiency and accuracy of detection, has a good application scenario.

HIROSE[1] et al. have developed the THES series of wheeled pipeline robots, which can carry a miniature camera to move rapidly in small diameter pipelines; Korea Aerospace University has developed a bionic pipeline robot[2], which imitates earthworm writhing and is driven by pneumatic pressure and can travel at a speed of 50mm/s, but has poor load capacity, short distance and can only move in one direction. KIM[3-5] et al. developed MRINSPECT series of wheeled pipeline robots and apply differential wheel systems to pipeline robots. The bionic pipeline inspection robot designed by the National University of Defense Technology[6] has a large driving force, but does not have vertical pipeline walking capability and has poor cornering performance. Tang Dewei et al.[7] developed a wheeled pipeline robot with differential motion capability, and the robot can automatically adjust the drive wheel speed through the differential mechanism when cornering. Yan Hongwei et al. developed a fully driven-wheeled pipeline robot and performed a kinematic analysis of the robot's bending[8,9].

At present, the research on small-diameter pipeline robots is mainly in the laboratory stage and cannot be applied in industrial production[10].

The above pipeline inspection robot has problems such as the inability to walk in vertical pipelines, poor passability of 90° bends, and difficulty in control. In this paper, a small-diameter pipeline inspection robot is designed for the pipeline environment and characteristics of DN100 in the gathering station, and the rationality and feasibility of the robot structure design are verified by using dynamics simulation and combining it with a prototype test.

## 2. Mechanical structure

In order to facilitate the installation and disassembly of the pipeline robot, the modular design idea is adopted to divide the drive module that provides power into three small modules: drive mechanism, reducing mechanism, and support mechanism, as shown in Figure 1. The three identical drive and reducing mechanisms are evenly distributed on the support mechanism at 120° circumferential direction.

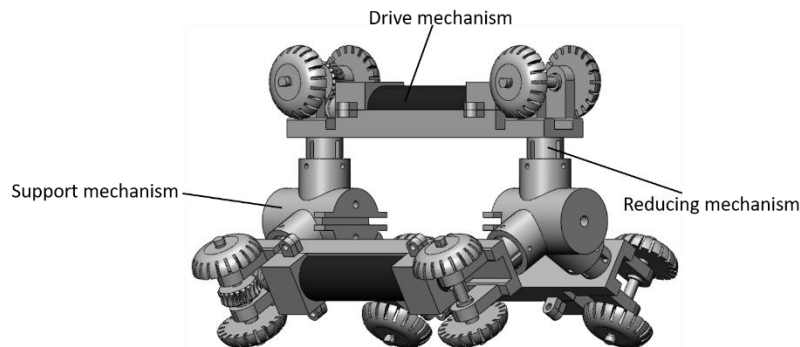


Figure 1: Pipeline robot structure composition

Each drive mechanism is driven by an independent servo motor. In order to improve the robot's bending ability, a worm gear is adopted as the drive structure of the drive mechanism under the requirement of meeting the movement speed. By reducing the height between the front and rear wheels, the resistance with the inner side of the pipe wall when it bends is avoided, which leads to failure to bend. The wheels are designed to be rounded and patterned on the wheels, which can not only increase the contact area with the inner wall of the pipe but also increase friction to avoid wheel slippage.

The reducer mechanism adopts the spring reducer method, which can adapt to the complex environment in the pipe in real time.

## 3. Cornering geometry analysis and kinematic analysis

### 3.1. Two or more

To ensure the smooth bending of the pipeline robot, a geometric analysis of the maximum length and width of the pipeline robot is required. The robot has the following two cases in the process of bending, as shown in Figs.2 and 3. Simplifying the robot as a cylinder [11], let the inner diameter of the pipe be  $D$ , the radius of curvature of the bend be  $R$ , the bending angle of the pipe be  $\alpha$ , the length of the pipe robot is  $L$ , and the width of the pipe robot is  $d$ .

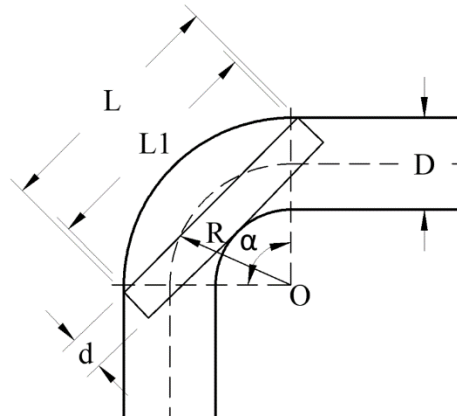


Figure 2: The body of the pipe robot is too long

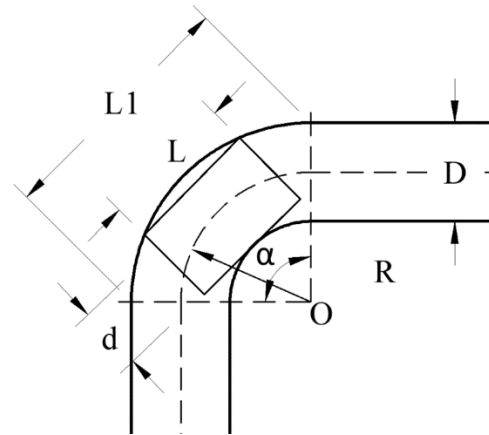


Figure 3: The body of the pipe robot is too thick

The geometrical constraints of the robot for cornering shall be in accordance with the following conditions.

$$\left(R + \frac{D}{2}\right) \cdot \cos\left(\frac{\alpha}{2}\right) - \left(R - \frac{D}{2}\right) \geq 0 \tag{1}$$

For the states shown in Figure 2.

$$\begin{cases} 0 < d < \left(R + \frac{D}{2}\right) \cdot \cos\left(\frac{\alpha}{2}\right) - \left(R - \frac{D}{2}\right) \\ L_{max} = \left(R + \frac{D}{2}\right) \cdot \cos\left(\frac{\alpha}{2}\right) - \left(R - \frac{D}{2}\right) \cos\left(\frac{\alpha}{2}\right) \end{cases} \tag{2}$$

For the states shown in Figure 3.

$$\begin{cases} 0 < d < D \\ L_{max} = 2 \cdot \sqrt{\left(R + \frac{D}{2}\right)^2 - \left(R - \frac{D}{2} + \frac{d}{2}\right)^2} \end{cases} \tag{3}$$

According to equations (1)-(3), the maximum length limit of the pipe robot design is finally determined  $L \leq 280mm$ , to prevent the pipe robot from getting stuck in the bend due to being too long or too thick length, the pipe robot length  $L=115mm$  is designed in this paper.

### 3.2. Motion analysis

The radius of curvature of each wheel's contact point with the inner wall of the pipe is different during the pipe robot's turning process. Therefore, in order to avoid the internal consumption caused by the speed mismatch of each wheel, the motion of the pipe robot in the bend should rotate around the center of curvature of the bend. To pass through the bend smoothly, two states of motion must be experienced: the transition phase and the rotation phase. Assuming the center of curvature of the pipe bend as the origin, the X-axis is positive in the direction of robot travel, and the Y-axis is positive in the vertically upward direction, the global coordinate system  $O_0(X_0, Y_0, Z_0)$  is shown in Figure 4.

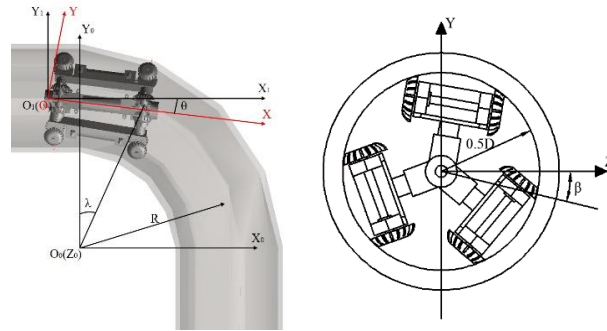


Figure 4: Schematic diagram of robot entering the bend

### 3.2.1. Transition phase motion analysis

The process of a pipe robot going from a straight pipe into a bend or from a bend into a straight pipe is called the transition phase. Let the wheel center distance between the front and rear ends be  $w$ ,  $\theta$  be the rotation angle of the robot coordinate system,  $\lambda$  be the angle that the center of the front face of the robot turns through during the bend, and  $\beta$  is the attitude angle of the robot, and the coordinates of the twelve contact points between the front and rear wheel systems of the pipe robot and the inner wall of the pipe in mutual contact in the local coordinate system  $O(X, Y, Z)$  can be expressed as follows respectively ( $s$  and  $c$  are used in the matrix instead of  $\sin$  and  $\cos$ , respectively)

$$Front=(f_1, f_2, f_3, f_4, f_5, f_6)= \begin{bmatrix} \frac{w}{2} \cdot s\beta & \frac{w}{2} \cdot s(240^\circ + \beta) & -\frac{w}{2} \cdot s(120^\circ + \beta) & \frac{w}{2} \cdot s\beta & -\frac{w}{2} \cdot s(240^\circ + \beta) & \frac{w}{2} \cdot s(120^\circ + \beta) \\ \frac{w}{2} \cdot c\beta & -\frac{w}{2} \cdot c(240^\circ + \beta) & \frac{w}{2} \cdot c(120^\circ + \beta) & -\frac{w}{2} \cdot c\beta & \frac{w}{2} \cdot c(240^\circ + \beta) & -\frac{w}{2} \cdot c(120^\circ + \beta) \end{bmatrix} \quad (4)$$

$$Back=(b_1, b_2, b_3, b_4, b_5, b_6)= \begin{bmatrix} 0 & 0 & 0 & 0 & 0 & 0 \\ -\frac{D}{2} \cdot s\beta & \frac{D}{2} \cdot s(240^\circ + \beta) & -\frac{D}{2} \cdot s(120^\circ + \beta) & \frac{D}{2} \cdot s\beta & -\frac{D}{2} \cdot s(240^\circ + \beta) & \frac{D}{2} \cdot s(120^\circ + \beta) \\ \frac{D}{2} \cdot c\beta & -\frac{D}{2} \cdot c(240^\circ + \beta) & \frac{D}{2} \cdot c(120^\circ + \beta) & -\frac{D}{2} \cdot c\beta & \frac{D}{2} \cdot c(240^\circ + \beta) & -\frac{D}{2} \cdot c(120^\circ + \beta) \end{bmatrix} \quad (5)$$

where: matrix  $f_1, f_2, f_3, f_4, f_5, f_6$  and  $b_1, b_2, b_3, b_4, b_5, b_6$  are the coordinate values of the contact points between the front and rear wheels and the pipe wall, respectively.

The rotation transformation matrix from the transition coordinate system  $O_1(X_1, Y_1, Z_1)$  to the local coordinate system  $O(X, Y, Z)$  is

$$R_1 = Rot(Z_1, -\theta) = \begin{bmatrix} \cos\theta & \sin\theta & 0 \\ -\sin\theta & \cos\theta & 0 \\ 0 & 0 & 1 \end{bmatrix} \quad (6)$$

The translation vector from the global coordinate system  $O_0(X_0, Y_0, Z_0)$  to the transition coordinate system  $O_1(X_1, Y_1, Z_1)$  is

$$T_0 = \begin{bmatrix} R\sin\lambda - \sqrt{w^2 - R^2(1 - \cos\lambda)^2} \\ R \\ 0 \end{bmatrix} \quad (7)$$

According to the geometric relationship, there are

$$w\sin\theta = R(1 - \cos\lambda) \quad (8)$$

Therefore, the coordinates of the contact points between the front and rear wheel systems of the robot and the pipe wall are described in the global coordinate system as

$$\begin{cases} F = R_1 Front + T \\ B = R_1 Back + T \end{cases} \quad (9)$$

where T is the translation matrix

$$T = [T_0 \ T_0 \ T_0 \ T_0 \ T_0 \ T_0] \tag{10}$$

The velocity of the wheel in the X, Y, and Z directions of the global coordinate system is obtained by deriving the Front and Back time components as

$$V_F = \begin{bmatrix} v_{fx1} & v_{fx2} & v_{fx3} & v_{fx4} & v_{fx5} & v_{fx6} \\ v_{fy1} & v_{fy2} & v_{fy3} & v_{fy4} & v_{fy5} & v_{fy6} \\ v_{fz1} & v_{fz2} & v_{fz3} & v_{fz4} & v_{fz5} & v_{fz6} \end{bmatrix} \tag{11}$$

Therefore the magnitude of the velocity of the front and rear wheels of the pipeline robot at the point of contact with the pipe wall is (i = 1, 2, 3, 4, 5, 6)

$$\begin{cases} v_{fi} = \sqrt{v_{fxi}^2 + v_{fyi}^2 + v_{fzi}^2} \\ v_{bi} = \sqrt{v_{bxi}^2 + v_{byi}^2 + v_{bzi}^2} \end{cases} \tag{12}$$

Therefore, in order to reduce the internal consumption of the pipeline robot in the transition phase, the speed between the front wheels of the robot should be changed indirectly by controlling the output torque of the servo motor to increase the smoothness of the motion of the pipeline robot during cornering.

### 3.2.2. Rotational phase motion analysis

The state in which the pipe robot enters the bend completely is called the rotation phase. Since the front and rear wheel systems of the robot move in the rotation phase in exactly the same state, only one set of wheel systems needs to be analyzed. As the pipeline robot rotates around the  $O_z$  axis, the velocity at the contact point between each module and the bend is proportional to the corresponding radius of curvature, resulting in a smooth passage of the pipeline robot. Thus, the velocity coordination model of the robot during the rotation phase[12] is

$$n_1:n_2:n_3:n_4:n_5:n_6 = R_1:R_2:R_3:R_4:R_5:R_6 \tag{13}$$

In equation (13), the  $n_i$  and  $R_i$  are respectively the first  $i$  speed of the whole wheel, the  $i$  radius of curvature of the contact point between the wheel as a whole, and the inner wall of the pipe (i = 1, 2, 3, 4, 5, 6).

## 4. Simulation analysis

The pipeline robot is modeled using 3D software and imported into the dynamics simulation software. Firstly, material properties are given to each part, and constraints such as moving, rotating, and fixed subsets are added between each part; secondly, spring constraints and contact forces between wheels and pipe walls are added by setting parameters such as spring stiffness and friction coefficient; Finally, rotating drives are added for motion simulation analysis.

### 4.1. Vertical pipe simulation

The vertical pipeline is an important part of the pipeline system in the oil and gas gathering and transmission site, so the designed robot drive module is simulated and analyzed for vertical walking capability. From Fig. 5, it can be seen that the robot's speed becomes negative at first due to the effect of gravity, and then returns to a positive value after the preload force is fully loaded.

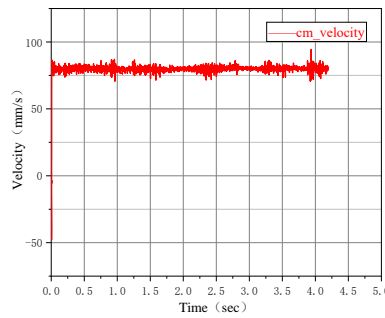


Figure 5: Velocity-time curve of the robot in the vertical tube

### 4.2. Curve Simulation

The robot drive module pass-through simulation was carried out in a pipe bend with pipe diameter  $D=100\text{mm}$  and  $1.5D$  radius of curvature, and the simulation results are shown in Figure 6. From Fig. 7, it can be seen that during the bending process, the existence of the compression spring can make the robot always contact with the pipe wall, so that it has good motion stability.

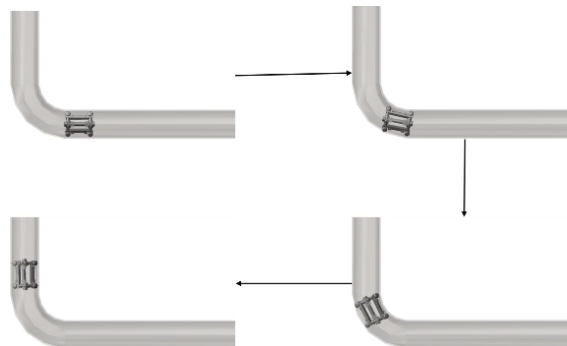


Figure 6: Robot cornering process

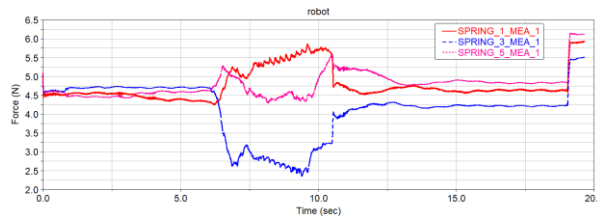


Figure 7: Spring force curve

## 5. Experimental validation

A straight pipe with a pipe diameter of 100 mm was combined with a  $90^\circ$  elbow with a radius of curvature of 1.5 times the pipe diameter to form the test pipe, as shown in Figure 8. The prototype production was adopted for 3D printing, as shown in Figure 9.



Figure 8: Test pipe

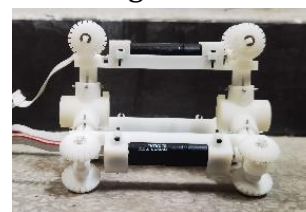


Figure 9: Prototype model

### 5.1. Vertical pipe feasibility test

In order to verify the feasibility of the drive module in a vertical pipe, a test was conducted as shown in Fig. 10. The test results showed that the robot itself could remain stationary and not



fall when no power was given to the robot; when power was given to the robot, vertical walking could be achieved.

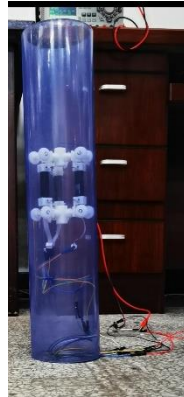


Figure 10: Vertical tube walking test

## 5.2. Bend passability test

A horizontal 90° bend was selected to verify the bending-through performance of the robot. Figure 12 shows the motion of the robot in the bent pipe, where (a) represents the straight pipe stage, (b)-(d) represents the over-bending stage, and (e) represents the straight pipe stage.

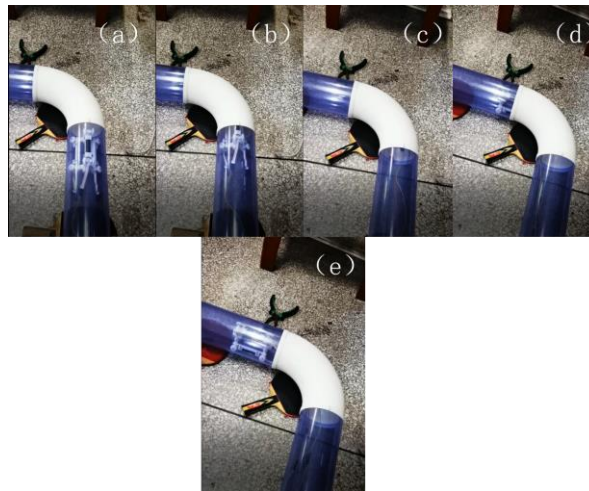


Figure 9: Bend passability test

## 6. Conclusion

A small-diameter pipeline inspection robot drive module is designed for the pipeline diameter of DN100 in the oil and gas gathering and transmission station. The simulation and experiment show that the robot can walk in the vertical pipeline and pass through the 90° bend with 1.5 times the radius of curvature, which initially verifies the feasibility of the design.

In subsequent work, the remaining modules will be combined to make a more fully functional pipeline inspection robot and to verify its detection results.

## References

- [1] HIROSE S, OHNO H, MITSUI T, et al. Design of In-pipe Inspection Vehicles for  $\Phi 25$ ,  $\Phi 50$ ,  $\Phi 150$  pipes[C]// Proceedings 1999 IEEE International Conference on Robotics and Automation, May 10-15, 1999, Detroit, USA. New York: IEEE, 1999:2309-2314.
- [2] Lim J W, Park H, An J, et al. One Pneumatic Line Based Inchworm-like Micro Robot for Half-inch Pipe Inspection[J]. Mechatronics, 2008, 18: 315-322.

- [3] YANG S U, KIM H M, SUH J S, et al. Novel robot mechanism capable of 3D differential driving inside pipelines[C]// 2014 IEEE/RSJ International Conference on Intelligent Robots and Systems, Sept. 14-18, 2014, Chicago, USA. new York: IEEE, 2014: 1944-1949.
- [4] KIM H M, YUN S C, LEE Y G, et al. Novel mechanism for in-pipe robot based on a multiaxial differential gear mechanism[J]. IEEE/ASME Transactions on Mechatronics, 2017, 22(1): 227-235.
- [5] KIM H M, YANG S U, YUN S C, et al. Design of back-drivable joint mechanism for in-pipe robot [C]// 2015 IEEE/RSJ International Conference on Intelligent Robots and Systems, Sept. 28-Oct. 2, 2015, Hamburg, Germany. new York: IEEE, 2015: 3779-3784.
- [6] Xie XH, Wang HG, Xu CQ. Mechanism Design and Dynamics Analysis on Micro-pipe Robot[J]. Journal of the National University of Defense Technology.2007,29(6):98-101.
- [7] Tang D.W., Li Q.K., Jiang S.Y., et al. Design and Analysis of a Pipeline Robot with the Function of Differential Movement[J]. Journal of Mechanical Engineering,2011,47(13).
- [8] Yan H.W., Wang Y, Ma J.Q., et al. Analysis for Dynamic Characteristics of Wheeled Pipe Robot in Elbow[J]. Journal of Xi'an Jiaotong University, 2018,52(8):87-94.
- [9] Xie T.Y., Li Q., Ding Y.W., Sun L. Design and Analysis of a Multi-Module Snake Shaped Pipeline Grinding Robot[J]. Robot, 2020, 42(06): 672-685.
- [10] Wang Yaohua, Zuo Rengui. Status of research on tiny pipeline robots at home and abroad[J]. Mechanical Design,2010,27(12):1-5,17.
- [11] Li Zhiqiang,Li Weiguo,Feng Zhicheng,Wang Lili,Yan Wengang,Guo Shijie.Structural and Passability Analysis of Pipeline Robot[J]. Mechanical Transmission,2021,45(06): 146-152.
- [12] CHEN Xiao,WU Zhipeng,HE Siyu,XIAO Xiaohui.Passing property design of adaptive support pipeline detection robot[J]. Journal of Central South University (Natural Science Edition),2018,49(12):2953-2962.